Projections of atmospheric soluble iron deposition under CMIP6 emission scenarios.

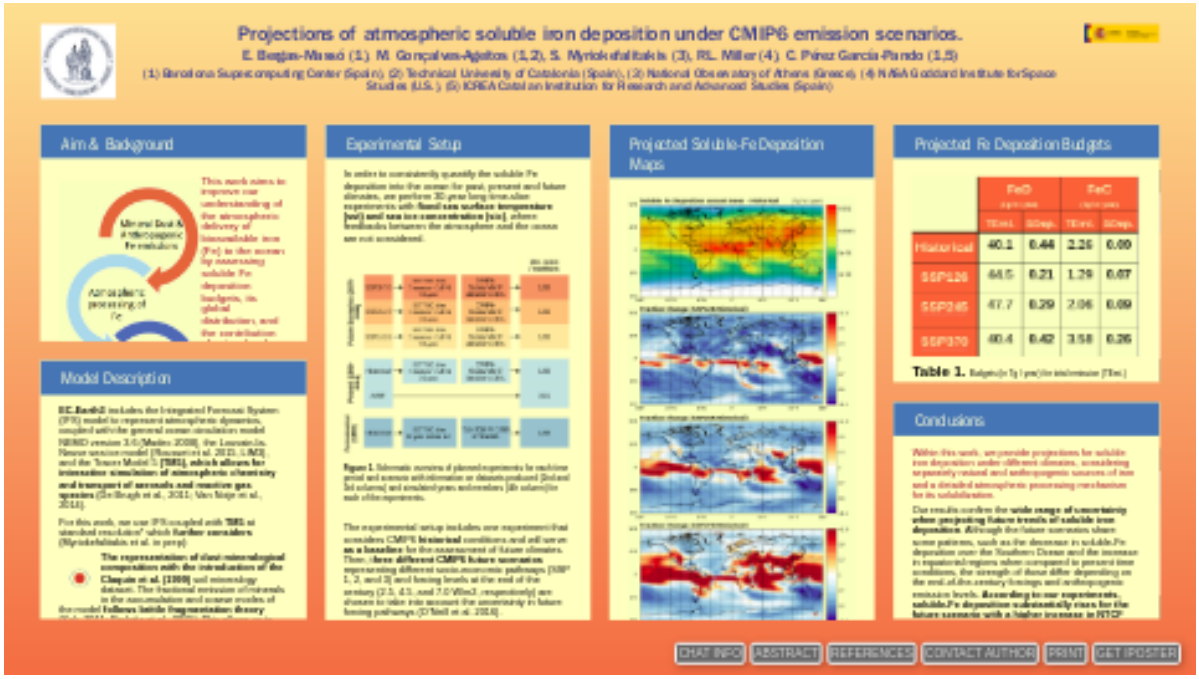

E. Bergas-Massó (1), M. Gonçalves-Ageitos (1,2), S. Myriokefalitakis (3), RL. Mi SHARE POSTERIler (4), C. Pérez García-Pando (1,5)

(1) Barcelona Supercomputing Center (Spain), (2) Technical University of Catalonia (Spain), (3) National Observatory of Athens (Greece), (4) NASA Goddard Institute for Space Studies (U.S.), (5) ICREA Catalan Institution for Research and Advanced Studies (Spain)

European Research Council

AXA Research Fund

PRESENTED AT:

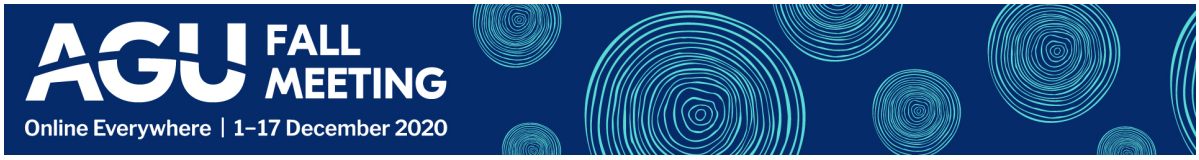

AIM & BACKGROUND

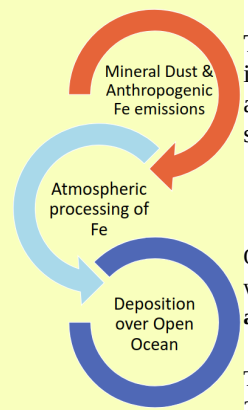

This work aims to improve our understanding of the atmospheric delivery of bioavailable iron (Fe) to the ocean by assessing soluble Fe deposition budgets, its global distribution, and the contribution of natural and anthropogenic sources under different climate scenarios.

Ocean productivity relies upon bioavailable Fe for photosynthesis, respiration, and nitrogen fixation, which makes the **Fe biogeochemical cycle a key modulator of the ocean's ability to uptake atmospheric CO2** (Ciais et al. 2013).

The **main external input of Fe to the open ocean** surface is atmospheric deposition (Jickells et al. 2005), which derives mainly from:

- **Soil dust aerosols** transported from arid and semi-arid regions (**~95%**).
- Fe-containing **aerosols from biomass burning and anthropogenic combustion** processes (**~5%**).

Fe in freshly emitted soil dust is mostly insoluble, but it is hypothesized to be partly transformed into bioavailable Fe species during atmospheric transport through a variety of **dissolution mechanisms, controlled** to a large extent **by atmospheric composition**.

The effects on the iron cycle of an increasing human activity since the Industrial Revolution and its future trends have been barely explored. Despite large uncertainties, it is accepted that the rise in anthropogenic combustion emissions has increased the iron atmospheric burden along with the acidity of the atmosphere, which further fosters iron solubilization (e.g. Shi et al., 2011). Changes in the natural dust cycle, and the associated iron emissions, are even more uncertain.

In this work, we present soluble Fe deposition calculations under present-day and different future climate conditions, conducted with a state-of-the-art Earth System Model (ESM), EC-Earth version 3, accounting for natural and anthropogenic iron sources as well as for atmospheric processing mechanisms.

MODEL DESCRIPTION

EC-Earth3 includes the Integrated Forecast System (IFS) model to represent atmospheric dynamics, coupled with the general ocean circulation model NEMO version 3.6 (Madec 2008), the Louvain-la-Neuve sea ice model (Rousset et al. 2015, LIM3), and the Tracer Model 5 **(TM5), which allows for interactive simulation of atmospheric chemistry and transport of aerosols and reactive gas species** (De Brugh et al., 2011; Van Noije et al., 2014).

For this work, we use IFS coupled with **TM5** at standard resolution* which **further considers** (Myriokefalitakis et al. in prep):

The representation of dust mineralogical composition with the introduction of the Claquin et al. (1999) soil mineralogy dataset. The fractional emission of minerals in the accumulation and coarse modes of the model **follows brittle fragmentation theory** (Kok, 2011; Perlwitz et al., 2015). This allows us to explicitly account for key minerals during the dissolution process

The primary emissions of both insoluble and soluble Fe forms, associated with mineral dust (Myriokefalitakis et al., 2018, 2015) **and combustion aerosols** (Ito et al, 2018). A percentage content in Fe and soluble Fe of the different Fe-containing minerals of dust is established (Nickovic et al., 2013). Scaling factors of Fe emissions to those of black carbon and organic carbon based on emission estimates (Ito et al. 2018) are applied for each of the emission sectors in CMIP6 corresponding to anthropogenic and biomass burning sources.

Explicit calculation of aqueous-phase chemistry of oxalate (OXL) and dissolution processes due to atmospheric acidity and organic ligands for both accumulation and coarse mode (Myriokefalitakis et al., 2015, 2018):

The thermodynamic equilibrium model **ISORROPIA II** (Fountoukis and Nenes, 2007) is used to estimate the water content and the acidity of hygroscopic aerosols for both the accumulation and coarse modes.

The atmospheric processing mechanism of iron treated as a kinetic process accounting for:

1) Proton-promoted dissolution

2) Oxalate-promoted Fe dissolution (with **oxalate calculated on-line**)

3) Photo-reductive dissolution.

*The chemistry module (TM5) uses a horizontal resolution of 3º in longitude by 2º in latitude, with 34 hybrid layers up to 0.1 hPa and the atmospheric module, IFS, follows the standard T255L91 resolution (which corresponds to approximately 0.75º in the horizontal and 91 vertical layers).

EXPERIMENTAL SETUP

In order to consistently quantify the soluble Fe deposition into the ocean for past, present and future climates, we perform 30-year long time-slice experiments with **fixed sea surface temperature (sst) and sea ice concentration (sic)**, where feedbacks between the atmosphere and the ocean are not considered.

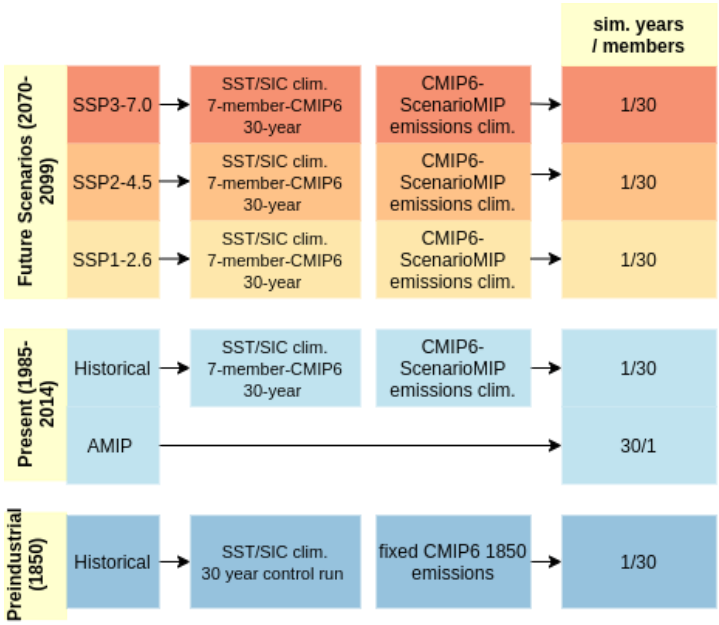

Figure 1. Schematic overview of planned experiments for each time period and scenario with information on datasets produced (2nd and 3rd columns) and simulated years and members (4th column) for each of the experiments.

The experimental setup includes one experiment that considers CMIP6 **historical** conditions and will serve **as a baseline** for the assessment of future climates. Then, t**hree different CMIP6 future scenarios** representing different socio-economic pathways (SSP 1, 2, and 3) and forcing levels at the end of the century (2.5, 4.5, and 7.0 W/m2, respectively) are chosen to take into account the uncertainty in future forcing pathways (O'Neill et al. 2016).

SSP3-7.0: medium to high end of the range of future forcing pathways with high near-term climate forcers (NTCF) emissions.

SSP2-4.5: business as usual scenario that falls in the **medium** part of the range of future forcing pathways and NTCF emissions.

SSP1-2.6: optimistic and sustainable pathway, that lies in the **low** end of the range of future forcing pathways and NTFC emissions.

The methodology used to set up those simulations is as follows:

1. Produce climatological sst and sic for each of the scenarios based on 30-years of coupled atmosphere-ocean experiments conducted with EC-Earthv3 and available in the CMIP6 repository. The periods selected are: **future scenarios 2070-2099, present historical 1985-2014, and fixed 1850 for preindustrial.**
2. Produce equivalent climatologies from ScenarioMIP emissions (Gidden et al. 2019)
3. Each experiment relies on 30 1-year-long members with those prescribed ocean climatologies and emissions, which consider initial conditions from a 2 year-long spin-up and apply slight perturbations for the atmospheric variables, so as to sample the climate variability.

PROJECTED SOLUBLE-FE DEPOSITION MAPS

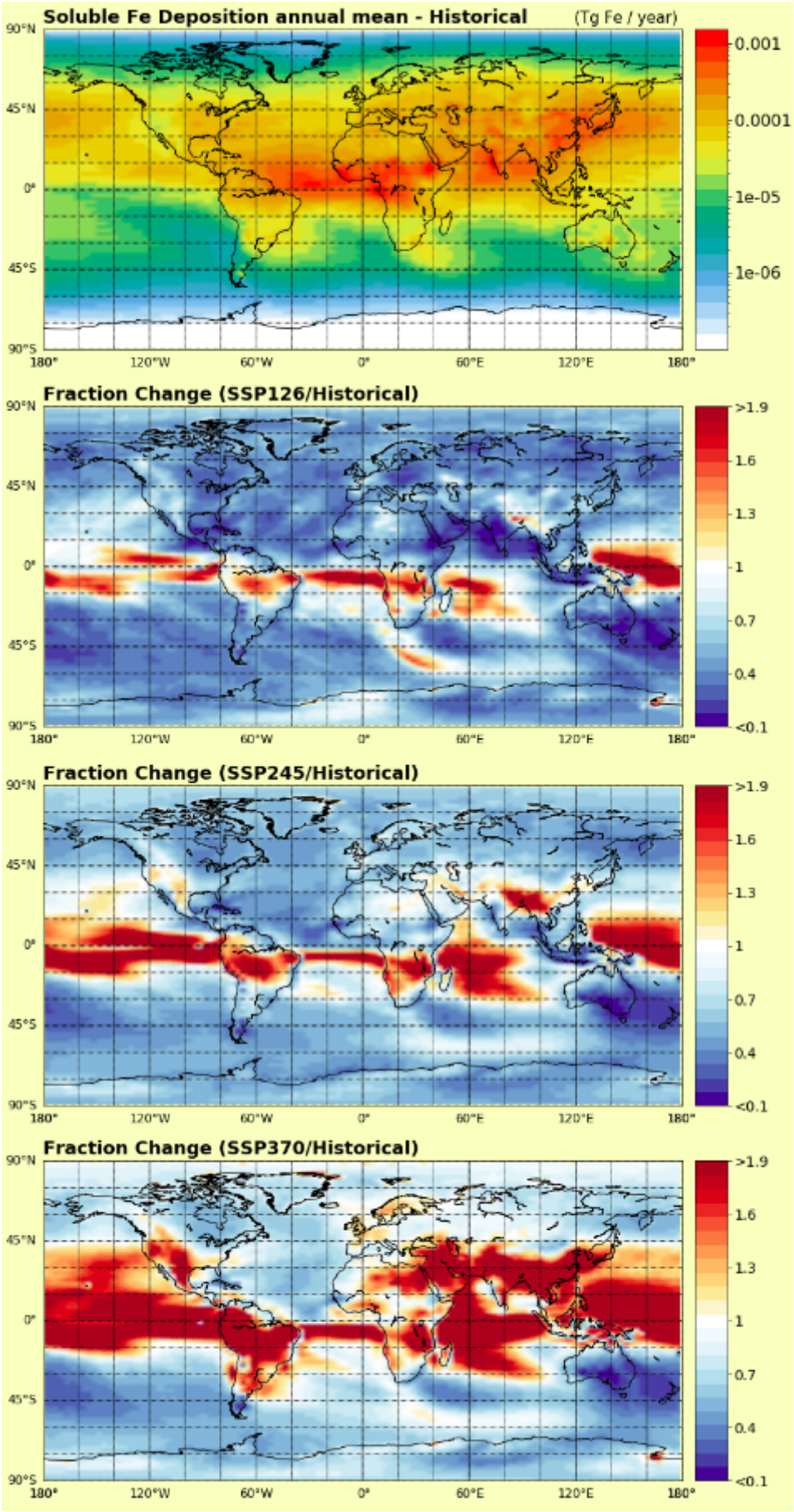

Figure 2. Soluble Fe deposition (Tg Fe / year) for historical scenario (top) and fractional changes between SSP126, SSP245, SSP370 and historical from top to bottom, respectively.

In the **historical period, the largest soluble Fe deposition fluxes** (up to a flux of 0.001 Tg Fe / year) **occur over the equatorial Atlantic area** , which is known to be downwind of main dust-source regions and biomass burning areas of Central Africa. Overall the soluble Fe deposition budget in the North Hemisphere (NH) is larger than in the Southern Hemisphere as the dust belt is shifted towards the north and major anthropogenic emission areas are found there (e.g, East Asia). In the Southern Hemisphere (SH) main areas of soluble Fe deposition are downwind dust source regions such as Australia, South Africa or South America (Figure 2, top).

In all the future scenarios, those regions with larger deposition fluxes are boosted. For the most sustainable pathway (SSP126), we get a decrease in deposition overall the globe except for the equator. Same pattern is seen for SSP245, although deposition increases in the Indian Ocean and Asia with respect to SSP126. **We get the major increase in the equator with SSP370**, **suggesting that the signal gets stronger the higher the anthropogenic emissions and forcing are in a scenario.** Deposition over the Indian Ocean and Asia's Pacific coast also experiences a remarkable increase for SSP370 due to a sharp rise of anthropogenic emissions on East Asia, which has a double effect on Fe deposition: by increasing primary emissions and by fostering Fe solubilization, because of an increase in atmospheric acidity. On the other hand, **the Southern Ocean**, which is known to have large iron-limited areas, **experiences a substantial decrease in Fe soluble iron deposition for all future scenarios.** In contrast, in **other HNLC regions like the Northern Pacific, we project an increase for SSP370.**

PROJECTED FE DEPOSITION BUDGETS

	FeD (Tg Fe / year)		FeC (Tg Fe / year)	
	TEmi.	SDep.	TEmi.	SDep.
Historical	40.1	**0.44**	2.26	**0.09**
SSP126	44.5	**0.21**	1.29	**0.07**
SSP245	47.7	**0.29**	2.06	**0.09**
SSP370	40.4	**0.42**	3.58	**0.26**

Table 1. Budgets (in Tg / year) for total emission (TEmi.) and soluble deposition (SDep.) for Fe-fust (FeD), combustion Fe (FeC).

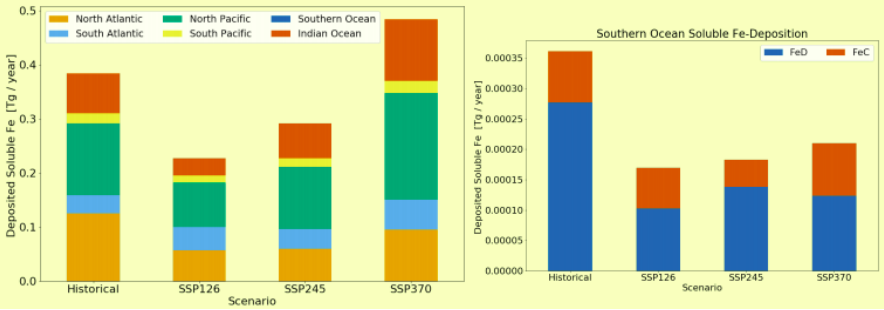

Figure 3. Deposited soluble Fe (Tg Fe/year) on different ocean basins (Vet et al, 2014) for the different scenarios (left) and details on soluble-Fe coming from dust sources (FeD) or combustion sources (FeC) for the Southern Ocean (right).

- Fe-dust emissions increase for the more optimistic future scenarios (SSP125, SSP245) compared to the historical period. For the SSP370, Fe-dust emissions remain in the same order of magnitude as those of the historical. **In spite of having less freshly Fe-dust emitted below the SSP370 and historical conditions, soluble Fe-dust deposition is larger compared to SSP126 and SSP245.** A more effective atmospheric solubilization could explain this behavior, due to higher combustion emissions and hence atmospheric acidity.

- **Fe-combustion emissions increase for the pessimistic future scenario (SSP370) which leads to a significant increase in soluble iron deposition** from combustion sources. On the other hand, **those emissions slightly decrease for SSP245 and sharply drop for SSP125** with respect to the historical simulation.

- **Total soluble-Fe deposition over oceans is higher in SSP370** with respect to the present-time, but also when compared to SSP126 and SSP245 scenarios.

- **Soluble-Fe deposition over the Southern Ocean** (Figure 3, right panel) which is known to be iron limited (Arteaga et al. 2020), **decreases for the three future scenarios with respect to present-time.** This decrease is explained by a reduction on SH dust-emissions and thus Fe in mineral dust in future scenarios.

Budgets in Table 1 fit overall well with prior studies results (Ito et al, 2019; Hamilton et al, 2020). However, our emission scenarios result in a lower soluble Fe deposition over the Southern Ocean which was not shown in previous works (Hamilton et al, 2020). The cause for the different behavior has to be further analyzed, but it could be attributed to differences on projected dust or biomass burning emissions.

CONCLUSIONS

Within this work, we provide projections for soluble iron deposition under different climates, considering separately natural and anthropogenic sources of iron and a detailed atmospheric processing mechanism for its solubilization.

Our results confirm the **wide range of uncertainty when projecting future trends of soluble iron deposition**. Although the future scenarios share some patterns, such as the decrease in soluble-Fe deposition over the Southern Ocean and the increase in equatorial regions when compared to present time conditions, the strength of those differ depending on the end-of-the-century forcings and anthropogenic emission levels. **According to our experiments, soluble-Fe deposition substantially rises for the future scenario with a higher increase in NTCF (SSP370, +50% with respect to present-time), while for the other future scenarios where Fe-combustion emissions are reduced with respect to present-time, soluble Fe-deposition decreases (-17% and -39% for SSP246 and SSP126, respectively)**. **Atmospheric acidity plays a fundamental role in the iron solubilization mechanisms,** and we show that even with lower total iron deposition burden (due to a decrease in soil-dust Fe), increased anthropogenic emissions lead to higher soluble deposition budgets (as shown in SSP370).

We have set a promising model baseline for EC-Earth accounting for an explicit representation of the atmospheric iron cycle that takes into consideration: primary Fe-emissions for anthropogenic, biomass burning and mineral dust emissions (where dust is on-line computed), an explicit calculation of aqueous-phase chemistry of OXL and dissolution processes due to atmospheric acidity and organic ligands. This would ultimately allow us fully coupled simulations accounting for ocean biogeochemistry. Further studies dealing with uncertainties that have not been discussed here as the effects on future land surface changes over dust and Fe emission or the use of different biomass burning emission databases will be considered.

Acknowledgments:

We thankfully acknowledge the computer resources at Marenostrum4, and the technical support provided by the Barcelona Supercomputing Center and the Computational Earth Sciences team of the Earth Sciences Department. This work was funded by the Ministerio de Conomía y Competitividad (MINECO) as part of the NUTRIENT project (CGL2017-88911-R). The research leading to this work has also recieved support by the ERC Consolidator Grant “FRAGMENT” (grant agreement No. 773051), and the AXA Chair on Sand and Dust Storms at BSC funded by the AXA research Fund. Finally, also acknowledge financial support for this work by the National Observatory of Athens research grant (no. 5065).

ABSTRACT

The **atmospheric supply of iron to the oceans** is fundamental to oceanic primary production and carbon dioxide uptake. Ocean productivity depends specifically upon the soluble or bioavailable fraction, which is poorly constrained by measurements. Recent studies suggest roughly a doubling of soluble iron deposition to the ocean since preindustrial climate conditions due to a combination of higher dust and combustion iron emissions along with more efficient atmospheric processing.

In our study, we will assess past, present, and future soluble iron deposition using an **advanced atmospheric iron cycle module implemented into the EC-Earth** Earth System Model. Mineral dust is calculated on-line considering an updated mineralogy dataset and particle size distribution at emission. The model takes into account primary emissions of insoluble and soluble Fe forms, associated with dust minerals and combustion aerosols. Dissolution processes due to atmospheric acidity and organic ligands, for both Fe-containing dust and combustion aerosols, are treated in the model as kinetic processes, accounting for 1) a proton-promoted, 2) an oxalate-promoted Fe dissolution (with oxalate calculated on-line), and 3) a photo-reductive dissolution. We run time-slice simulations using the atmosphere-chemistry model configuration using past, present, and future sea surface temperature and sea ice concentration climatologies obtained from EC-Earth CMIP6 coupled model experiments. We have chosen three different CMIP6 future scenarios representing different socio-economic pathways (SSP 1, 2, and 3) and different forcing levels by the end of the century (RCP 2.5, 4.5, and 7.0, respectively). We address the uncertainties attributed to the natural dust cycle, by perturbing the dust emissions in our past and future experiments. **Our setup allows estimating the soluble iron deposition into the ocean while quantifying the contribution from natural and anthropogenic sources under a range of scenarios.**

REFERENCES

Arteaga et al. (2020), Nat Commun 11, 5364.

Brugh et al. (2011), Atmos. Chem. Phys., 11, 1117–1139

Ciais et al. (2013), Carbon and other biogeochemical cycles. Climate Change 2013: The Physical Science Basis. 465-570.

Claquin et al. (1999), J. Geophys. Res., 104, 22243.

Fountoukis and Nenes (2007), Atmos. Chem. Phys., 7, 4639–4659.

Gidden et al. (2019), Geoscientific Model Development. 12. 1443-1475. 10.5194/gmd-12-1443-2019.

Ito et al. (2019), Sci. Adv., 5(5), eaau7671, doi:10.1126/sciadv.aau7671

Ito et al. (2018), Sci. Rep. 8, 7347.

Jickells et al. (2005), Science, 308, 67–71, doi: 10.1126/science.1105959.

Kok, Jasper. (2011), Proceedings of the National Academy of Sciences of the United States of America. 108. 1016-21.

Myriokefalitakis et al. (2015), Biogeosciences, 12, 3973–3992.

Myriokefalitakis et al. (2018), Biogeosciences Discussions. 1-50. 10.5194/bg-2018-285.

Nickovic et al. (2013), Atmos. Chem. Phys., 13, 9169–9181.

Noije et al. (2014), Geosci. Model Dev., 7, 2435–2475.

O'Neill et al. (2016), Geoscientific Model Development. 9. 3461-3482. 10.5194/gmd-9-3461-2016.

Perlwitz et al. (2015), Atmos. Chem. Phys., 15, 11629-11652, doi:10.5194/acp-15-11629-2015.

Rousset et al. (2015), Geoscientific Model Development Discussions. 8. 3403-3441. 10.5194/gmdd-8-3403-2015.

Shi et al. (2011), Global Biogeochem. Cycles, 25, GB2010.

Vet et al. (2014), Atmospheric Environment, 93:3-100.